

STRESS ANALYSIS FOR ADHESIVE BONDED SINGLE LAP JOINTS

ȘTEFAN Bianca Minodora, CROITORU Alexandru Theonel
Facultatea: Transporturi, Specializarea: Ingineria transporturilor, Anul de studii: II,
e-mail: bianca.stf0013@gmail.com
Conducători științifici: Prof .dr. ing. Ștefan SOROHAN
Sl. dr. ing. Dragoș-Alexandru APOSTOL

ABSTRACT: The analysis and modeling of an adhesive joint may include aspects of analytical, numerical and experimental studies. In this work a particular single lap joint is analyzed for two sets of adherents: aluminum alloy and mild steel and a commercial adhesive i.e. Bison for metals. First the analytical calculations are done using the classical relations of Goland and Reissner. Then, two finite element models were developed and simulated in static conditions using a linear elastic behavior of materials by Ansys code. A very good correlation of the stress distribution in adhesive and adherent were obtained using the analytical and numerical method. Finally, the same sets of adherents and the same adhesive were used to prepare specimens which were tested statically in the lab. This time the obtained results were under the expected behavior probably due to some lack of specimen preparations. Important discussions and interpretations of the results are detailed presented.

KEYWORDS: adhesive, adherents, bonded, single lap joint, finite element analysis.

1. Introducere

Glued assemblies have rapidly expanded in the transport industry with the advent of structural adhesives, i.e. with increased rigidity and strength and which successfully handle with the fatigue demands to which the resistance structure in the field of transport is subjected.

Structural adhesives are chemicals that are applied in a fluid or viscous state between specially prepared surfaces on two parts that need to be joined together. If it has been well designed and completed, the connection between the parts (adherents) is strong and durable after the adhesive has hardened. The importance of adhesives is growing because modern structures include components made of different materials that are easily and securely placed by gluing [1, 2].

The main factors that determine the integrity of an adhesive bonded assembly are [1]: selection of the most suitable adhesive, compatible with the materials of the adherents; geometry of the joint; preparation of gluing surfaces; strict quality control on the assembly line; monitoring the behavior of the joints during the operation of the products. The main advantages of using adhesives are: it is possible to harden different materials; the joint line (surface) is continuous and contributes to the stiffening of the structures as a whole; the stress distribution is more uniform than in the case of using rivets or screws; the weight of the structure increases less than in the case of mechanical assemblies (with metal fasteners); quality joints can be made both on small surfaces and on large overlapping areas; the finishing operations after the hardening of the adhesive are simple, easy to execute; proper design can ensure increased fatigue strength as well as vibration damping.

However, some limitations in the use of adhesive joints must be taken into account: choosing the right adhesive and preparing the surfaces are essential for making quality assemblies; excessive operating temperatures reduce the strength of the joints; the handling of the assembled parts must be done with special precautions during the hardening of the adhesive in order to maintain the relatively correct position; the resistance to the action of environmental factors is decisive for maintaining the integrity of the adhesive for a long time.

High strength adhesives, called structural adhesives, have shear strengths of 15 – 50 MPa, Young's modulus of 1300–4500 MPa and Poisson's ratio between 0.3 and 0.42 [1]. There are analytical relationships for design stage applicable to the most commonly used assemblies [1 – 4].

The present paper presents classical analytical relations of calculation for an overlapping glued joint. Then, for a series of specimens that were prepared and tested experimentally, the finite element method was used to verify the results obtained analytically and finally the results obtained experimentally are presented and critically discussed.

2. Analytic relations

The calculation of the bonded single lap joints can be done with several methods [4, 5], here the Goland and Reissner method was adopted [1, 6]. In Fig. 1,b the origin of the axis system is placed in the center of the median surface of the adhesive layer of thickness t_a . The overlap length is $l = 2c$, and the adherents are considered of the same material and with the same thickness t . The force acting on the unit of width is $p_b = F/b$. One considers elastic stresses and homogeneous and isotropic materials. For the Young's modulus and Poisson's ratio, the notations E and ν are used, for the adherent material, respectively E_a and ν_a , for the adhesive. The shear modulus of the adhesive can be evaluated with the relation $G_a = E_a/[2(1+\nu_a)]$. The local bending of the adherents (Fig. 1,b) induces in the adhesive both shear stresses τ_{xy} and peel stresses σ_y (normal on the middle surface of the adhesive layer).

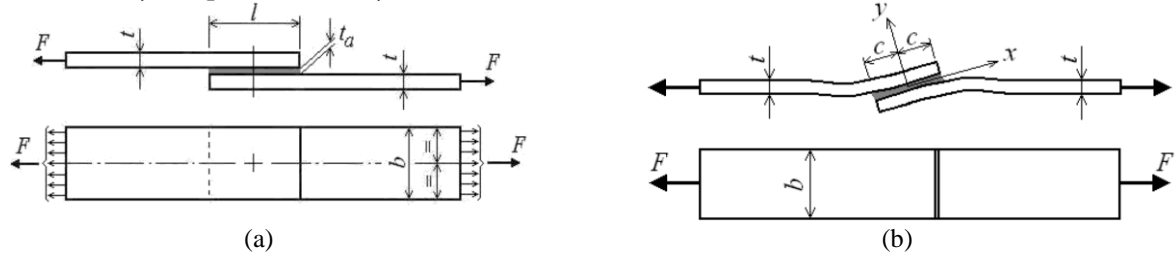


Fig. 1. Adhesive bonded single lap joint joint. (a) geometric parameter notations; (b) the Oxy coordinate system for the analytical description of stresses in the adhesive.

For shear stresses distribution one can use the relation

$$\tau_{xy}(x) = -\frac{p_b}{8c} \left[\frac{\beta c}{t} (1+3k) \frac{\cosh(\beta x/t)}{\sinh(\beta c/t)} + 3(1-k) \right], \quad (1)$$

where

$$\beta = \sqrt{8 \frac{G_a t}{E t_a}}; \quad k = \frac{\cosh(\chi c)}{\cosh(\chi c) + 2\sqrt{2} \sinh(\chi c)}; \quad \chi = \frac{1}{t} \sqrt{\frac{3p_b(1-\nu^2)}{2tE}}. \quad (2)$$

The peel stresses are described with the relation:

$$\sigma_y(x) = \frac{1}{\eta} \frac{p_b t}{c^2} \left[\left(R_2 \lambda^2 \frac{k}{2} + \lambda k_1 \cosh \lambda \cos \lambda \right) \cosh \frac{\lambda x}{c} \cos \frac{\lambda x}{c} + \left(R_1 \lambda^2 \frac{k}{2} + \lambda k_1 \sinh \lambda \sin \lambda \right) \sinh \frac{\lambda x}{c} \sin \frac{\lambda x}{c} \right], \quad (3)$$

where the next notations were used:

$$\lambda = \frac{c}{t} \sqrt[4]{6 \frac{E_a t}{E t_a}}; \quad k_1 = \frac{kc}{t} \sqrt{\frac{3p_b(1-\nu^2)}{tE}}; \quad \eta = \frac{1}{2} [\sinh(2\lambda) + \sin(2\lambda)]; \quad (4)$$

$$R_1 = \sinh \lambda \cos \lambda + \cosh \lambda \sin \lambda; \quad R_2 = \sinh \lambda \cos \lambda - \cosh \lambda \sin \lambda.$$

The maximum normal stress in the adherent due to the axial force and bending moment results

$$\sigma_{ad,max} = (1+3k) \frac{F}{bt} = (1+3k) \frac{p_b}{t}. \quad (5)$$

3. Finite element analysis and results presentation

Finite element analysis [7] allows much more accurate solutions to be obtained than analytical calculation. For this reason, a 2D plane stress model was developed for the dimension of the specimens that were prepared and tested experimentally, i.e. with two pairs of adherents: aluminum and steel (Fig. 2).

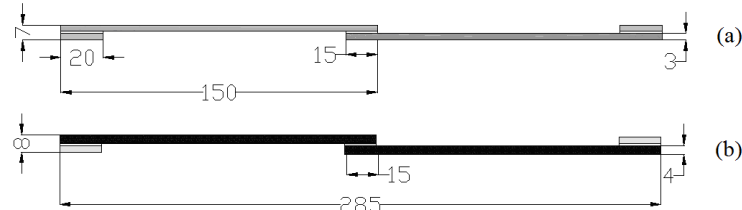


Fig. 2. Dimensions of experimentally tested specimens. The width of the specimens is $b = 25$ mm. (a) aluminum specimens; (b) steel specimens.

The finite element type Plane183 from Ansys was used for mesh, i.e. the quadrilateral element with 8 nodes and two degrees of freedom per node: displacements along the Ox and Oy axes. The models include over 20,000 nodes and around of 7,000 finite elements. The boundary conditions used in the simulation are specified in Fig. 3 and correspond to those in the experimental tests. The thickness of the adhesive was considered $t_a = 0.5$ mm and it was discretized much finer than the adherents. Because the numerical model is linear, the value of the load force F is not very important for stress distribution calculations. For both finite element models the same load $F = 1$ kN was chosen. The elastic material constants used in modeling are given in Table 1.

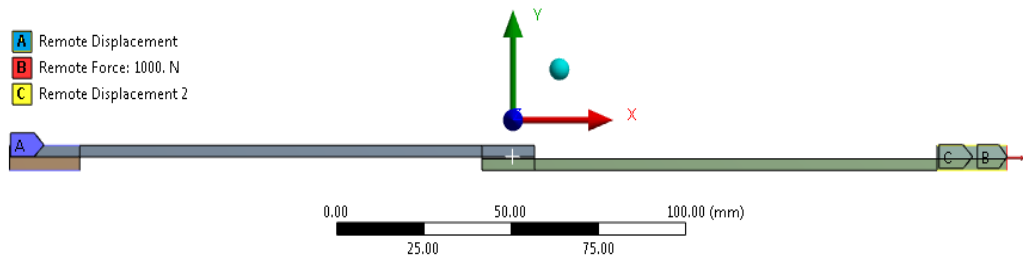


Fig. 3. Boundary conditions (load and supports) considered in the finite element models.

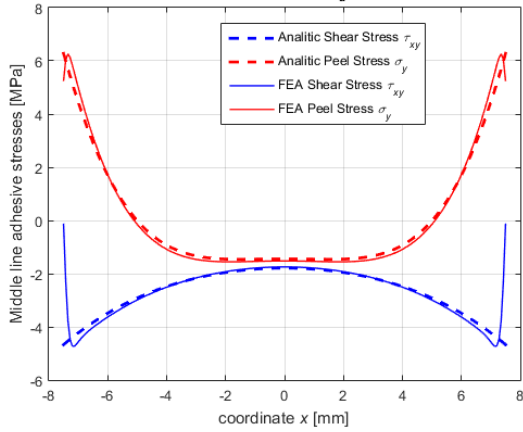
Table 1. Elastic properties of the materials.

Material	Young's modulus E [GPa]	Poisson's ratio ν [-]
Steel	200	0.3
Aluminum	70	0.33
Adhesive	1.85	0.38

The stress results in the median plane of the adhesive, obtained with the two developed finite element models, as well as the analytical ones using the relations (1)–(4) are presented in Fig. 4. The Matlab program was used to process the analytical relations. It is observed that the stress distribution obtained analytically is very close to the distribution obtained with the finite element method, which is considered more accurate in this case.

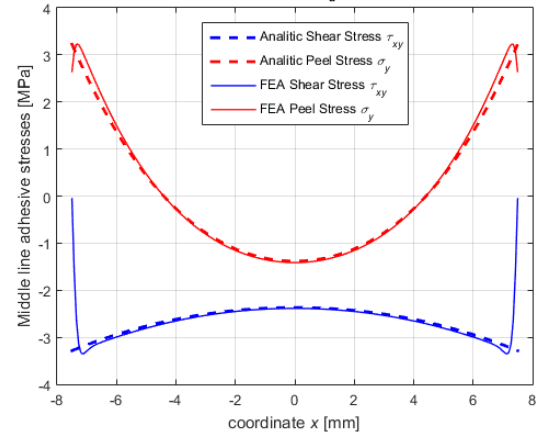
Using the relation (5), and the results obtained from the finite element analysis (FEA), respectively, in Table 2 the maximum stresses in the adherents, in the vicinity of the adhesive are presented. The probe stress in the finite element models was read at a distance t_a from the ends of the adhesive to remove the stress singularities at the adhesive roots.

Adherents: Aluminum; $l=15\text{mm}$; $t=3\text{mm}$; $t_a=0.5\text{mm}$; $b=25\text{mm}$; $F=1\text{ kN}$



(a)

Adherents: Steel; $l=15\text{mm}$; $t=4\text{mm}$; $t_a=0.5\text{mm}$; $b=25\text{mm}$; $F=1\text{ kN}$



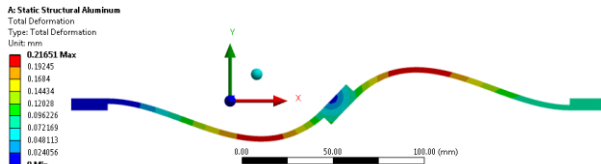
(b)

Fig. 4. Distribution of stresses in the median plane of the adhesive obtained analytically and with the finite element method for $F = 1\text{ kN}$. (a) aluminum adherents; (b) steel adherents.

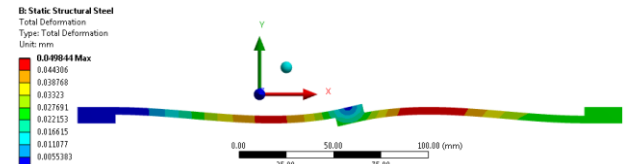
Table 2. Maximum normal stress (in MPa) in the adherents: $\sigma_{ad,max}$ when $F = 1\text{ kN}$.

Adherents	Analytic, relation (5)	FEA results in vicinity of adhesive layer (see Fig. 1,b)	Relative error [%]
Aluminum - Aluminum	49.3	53.1	7.15
Steel - Steel	38.7	40.3	3.97

The total displacement distributions and the deformed shapes of the finite element models are presented in Fig. 5. The von Mises stress distributions, including also the stress singularities, are accessible in Fig. 6. Here one can clearly observe the location of the maximum normal stress in the adherents. In Fig. 7, the von Mises stress distributions are presented only in the adhesive. Here it is very clear to observe some stress singularities at the ends of the adhesive layers.

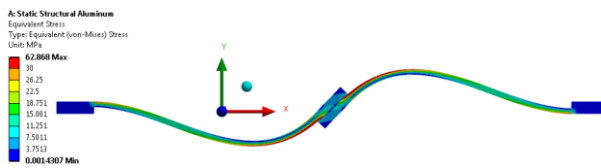


(a)

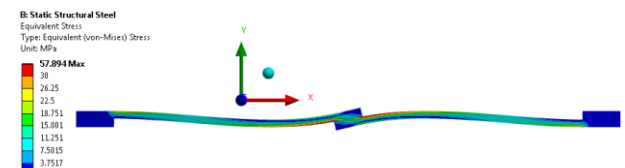


(b)

Fig. 5. Total displacement distributions if $F = 1\text{ kN}$. The deformed configuration is 100 times larger than the real ones. (a) aluminum adherents; (b) steel adherents.

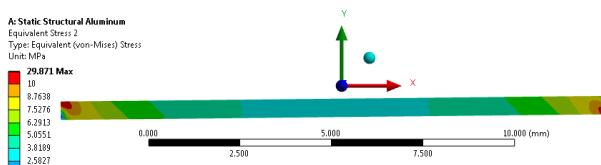


(a)

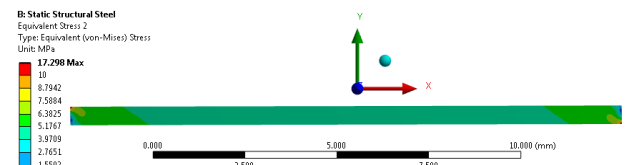


(b)

Fig. 6. Von Mises stress distributions if $F = 1\text{ kN}$. (a) aluminum adherents; (b) steel adherents.



(a)



(b)

Fig. 7. Von Mises stress distributions in adhesive only if $F = 1\text{ kN}$. (a) aluminum adherents; (b) steel adherents.

4. Experimental results

The experimental part focused on how to perform a laboratory test, following steps such as: procuring, cutting the material, removing burrs, sanding and decontamination of the surface, applying wax strips to maintain a 0.5 mm thick layer of adhesive, mixing and application of the two-component adhesive (BISON brand), pressing and curing time (48 hours in this case).

The static tensile test was performed at a speed of 1 mm/min using a Zwick Roell universal testing machine (Fig. 8) from a mechanical testing laboratory in the Strength of Materials department. Two sets of test pieces (specimens) were prepared and tested, each set consisting of three specimens. The lower end of the specimens is fixed and the traction force is applied to the upper one. The traction force and the displacement of the moving end are recorded during the tests. For the six created specimens, the characteristic curves are presented in Fig. 9. There is a relatively large dispersion of the results and the fact that the steel specimens take to a higher force than the aluminum ones. The maximum values of the registered forces, as well as the displacement of the free end at the moment of break are presented in Table 3.

Table 3. Experimental results

Adherents	Specimen No.	Global results	
		Maximum force [N]	Maximum displacement [mm]
Aluminum - Aluminum	1	1350	1.8
Aluminum - Aluminum	2	1350	1.3
Aluminum - Aluminum	3	359	0.8
Steel - Steel	4	1710	2.0
Steel - Steel	5	987	1.7
Steel - Steel	6	1800	2.2

The appearance of the specimens after the test is shown in Fig. 10, where it is observed that all breaks occurred by peeling off the adhesive from one of the adherents, which shows poor adhesion of the adhesive to the metal or the glued surfaces were not sufficiently well prepared for gluing.

Based on the characteristic curves obtained in the laboratory, a series of conclusions were drawn regarding the behavior of the adhesive. The characteristic curves obtained experimentally are similar to those obtained for textile yarns, i.e. hardening when the load increases. This apparently bizarre behavior may be due to the behavior of the adhesive in relatively low strength tests or other aspects unknown at first glance, which is why the tests should be repeated and optically monitored.



Fig. 8. Zwick Roell universal testing machine with aluminum-aluminum test specimen fitted for tensile testing.

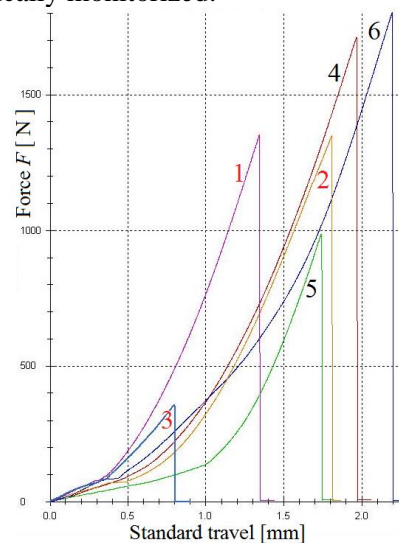


Fig. 9. The characteristic force-displacement curves obtained for all specimens tested. The figures next to the curves represent the test specimens according to Table 3.

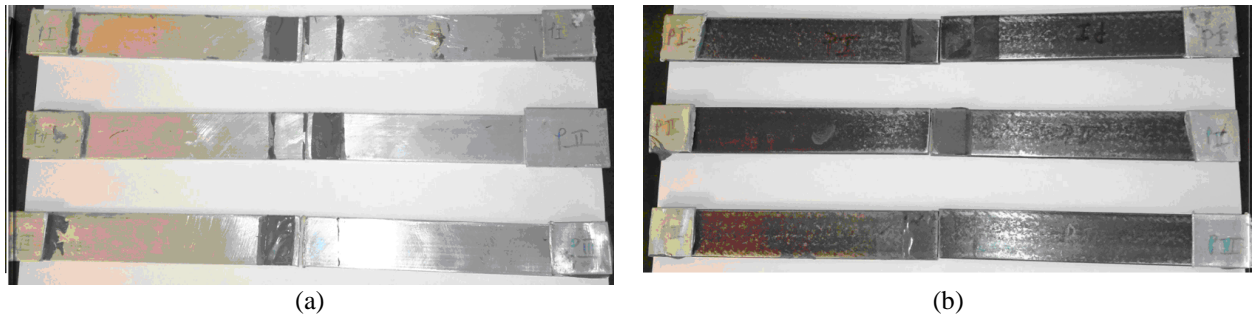


Fig. 10. Aspect of adherents after testing. (a) aluminum adherents; (b) steel adherents.

5. Conclusions

The study conducted in this paper shows that the Goland and Reissner relations [6], although obtained in 1944, can relatively correctly estimate the stress distribution and their maximum values.

Relatively rigid adhesives, which are marketed for individual use, in this case Bison [8], are not accompanied by all the elastic characteristics required in the calculation. For the two-component adhesive used in this paper, the manufacturer gives some more qualitative technical specifications. An adhesive strength of up to 22 MPa is guaranteed in the specifications without specifying the load type. Previous tests performed in the laboratory allowed partial characterization of this adhesive type and the data were used in modeling. However, for the tests performed and presented in this work, if the maximum strength obtained for the steel specimens $F_{\max} = 1.8$ kN is considered, then for the shear area $A_f = 15 \cdot 25 = 375$ mm², an average shear stress of 4.8 MPa results. This value is much lower than 22 MPa, but the yield for the tested specimens was not in the median plane of the adhesive, i.e. it did not yield but simply debonds because the adhesive does not have very good adhesion to metals. However, further investigation is required for extensive characterization of this adhesive.

6. References

- [1] Sandu, M., Sandu, A., Nuțu, E. (2019), *Rezistența materialelor*, Editura Printech, București, ISBN 978-606-23-0953-4.
- [2] Da Silva, L.F.M., Öchsner, A., Adams, R.D. (2018), *Handbook of adhesion technology*, 2nd edition. Heidelberg:Springer.
- [3] Da Silva, L.F., Campilho, R.D. (2012), *Advances in numerical modelling of adhesive joints*. Heidelberg: Springer.
- [4] Da Silva, L.F., das Neves, P.J., Adams, R., Spelt J. (2009), "Analytical models of adhesively bonded joints - Part I: Literature survey", *International Journal of Adhesion and Adhesives*; Vol. 29: pp. 319-30.
- [5] Sadeghi, M.Z., Gabener, A., Zimmermann, J., Savarana, K., Weiland, J., Reisinger, U., Schroeder, K.U. (2019), "Failure load prediction of adhesively bonded single lap joints by using various FEM techniques", *International Journal of Adhesion and Adhesives*, <https://doi.org/10.1016/j.ijadhadh.2019.102493>.
- [6] Goland, M., Reissner, E. (1944), "The stress in cemented joints", *Journal of Applied Mechanics*; No. 66: A17-A27.
- [7] Soroșan, Șt., (2015), *Elemente finite în ingineria mecanică-curs introductiv*, Editura Politehnica Press, București, ISBN 978-606-515-604-3.
- [8] <https://www.bison.net/en/product.6305443>.